

Strong-coupling Spin-singlet Superconductivity with Multiple Full Gaps in Hole-doped $\text{Ba}_{0.6}\text{K}_{0.4}\text{Fe}_2\text{As}_2$ Probed by ^{57}Fe -NMR

M. Yashima,^{1,2} H. Nishimura,¹ H. Mukuda,^{1,2} Y. Kitaoka,¹ K. Miyazawa,³
P. M. Shirage,³ K. Kiho,³ H. Kito,^{3,2} H. Eisaki,^{3,2} and A. Iyo^{3,2}

¹Graduate School of Engineering Science, Osaka University, Osaka 560-8531, Japan

²JST, TRiP, 1-2-1 Sengen, Tsukuba 305-0047, Japan

³National Institute of Advanced Industrial Science and Technology (AIST), Tsukuba, 305-8568, Japan

We present ^{57}Fe -NMR measurements of the novel normal and superconducting-state characteristics of the iron-arsenide superconductor $\text{Ba}_{0.6}\text{K}_{0.4}\text{Fe}_2\text{As}_2$ ($T_c = 38$ K). In the normal state, the measured Knight shift and nuclear spin-lattice relaxation rate ($1/T_1$) demonstrate the development of wave-number (q)-dependent spin fluctuations, except at $q = 0$, which may originate from the nesting across the disconnected Fermi surfaces. In the superconducting state, the spin component in the ^{57}Fe -Knight shift decreases to almost zero at low temperatures, evidencing a spin-singlet superconducting state. The ^{57}Fe - $1/T_1$ results are totally consistent with a s^\pm -wave model with multiple full gaps, regardless of doping with either electrons or holes.

The recent discovery of superconductivity (SC) in the iron (Fe)-based oxypnictide $\text{LaFeAsO}_{1-x}\text{F}_x$ at the SC transition temperature $T_c = 26$ K has provided a new route toward the realization of high- T_c SC [1]. The mother material, LaFeAsO , exhibits a structural phase transition from tetragonal (P4/nmm) to orthorhombic (Cmma) form at $T \sim 155$ K and then exhibits a striped antiferromagnetic (AFM) order with $\mathbf{Q} = (0, \pi)$ or $(\pi, 0)$ and $T_N \sim 140$ K [2]. The calculated Fermi surfaces (FSs) for undoped LaFeAsO consist of two small electron cylinders around the tetragonal M point and two hole cylinders, plus a heavy 3D hole pocket, around the Γ point [3]. Measurements of the nuclear spin-lattice relaxation rate ($1/T_1$) for the LaFeAsO system in the SC state revealed the lack of a coherence peak below T_c and the presence of T^3 -like behavior, suggesting an unconventional SC nature with line-node gaps [4, 5, 6]. However, some experiments to measure parameters such as penetration depth, together with studies using angle resolved photoemission spectroscopy (ARPES), have shown that the SC order parameter (OP) is of fully gapped s -wave symmetry [7, 8, 9, 10]. The theory was the first to propose s^\pm -wave pairing symmetry as a promising candidate for the SC state in Fe-pnictide superconductors [11, 12].

Another family of FeAs-based superconductors without oxygen has been reported in hole-doped $\text{Ba}_{1-x}\text{K}_x\text{Fe}_2\text{As}_2$ with $T_c = 38$ K [14]. The mother material, BaFe_2As_2 , has a ThCr_2Si_2 -type structure and consists of alternating layers comprising FeAs_4 tetrahedra and Ba. BaFe_2As_2 also exhibits a structural phase transition from the tetragonal (I4/mmm) to orthorhombic (Fmmm) form, accompanied by a striped AFM order with $\mathbf{Q} = (\pi, 0, \pi)$ at $T_N = 140$ K [15, 16]. The previous ^{75}As -NMR study on $\text{Ba}_{0.6}\text{K}_{0.4}\text{Fe}_2\text{As}_2$ reported that $1/T_1$ shows T^3 -like behavior well below T_c [17, 18], which is in contrast to the fully gapped

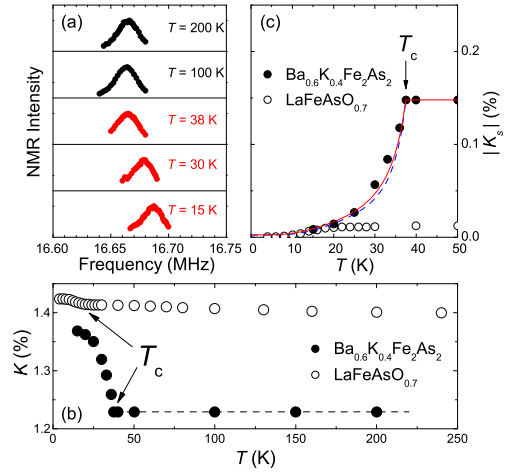


FIG. 1: (Color online) T dependence of (a) ^{57}Fe -NMR spectrum and (b) Knight shift (^{57}K) at $H = 11.966$ T parallel to the ab plane in $\text{Ba}_{0.6}\text{K}_{0.4}\text{Fe}_2\text{As}_2$. (c) The spin component $^{57}K_s$ in ^{57}K deduced by subtracting $K_{orb} \sim 1.38$ %, revealing a spin-singlet SC state similar to that in $\text{LaFeAsO}_{0.7}$ [23]. The solid and dashed lines indicate the calculated results assuming Model A and Model B with the same fitting parameters as those in $1/T_1$, respectively (see text).

s -wave symmetry of the SC OP, as revealed by ARPES on hole-doped $\text{Ba}_{0.6}\text{K}_{0.4}\text{Fe}_2\text{As}_2$ and electron-doped $\text{Ba}(\text{Fe}_{0.85}\text{Co}_{0.15})_2\text{As}_2$ [10, 19]. Furthermore, ARPES results for $\text{Ba}_{0.6}\text{K}_{0.4}\text{Fe}_2\text{As}_2$ show that there are two SC gaps with different values: a large gap on the two, small, hole-like and electron-like FS sheets, and a small gap on the large, hole-like FS [10]. This two-SC-gap phenomenon was suggested by NMR studies as well [20, 21]. In this letter, we report the results of microscopic ^{57}Fe -NMR measurements on hole-doped $\text{Ba}_{0.6}\text{K}_{0.4}\text{Fe}_2\text{As}_2$ with $T_c = 38$ K enriched with the isotope ^{57}Fe to address its normal-state and SC characteristics.

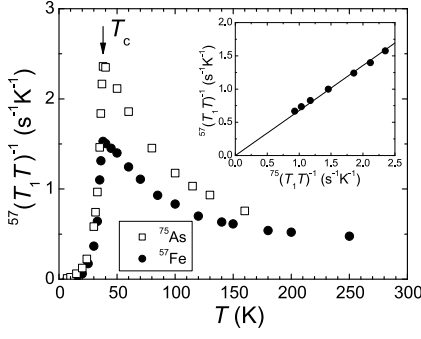


FIG. 2: (Color online) T dependence of $^{57}\text{Fe}-(T_1T)^{-1}$ in $\text{Ba}_{0.6}\text{K}_{0.4}\text{Fe}_2\text{As}_2$, along with that in $^{75}\text{As}-(T_1T)^{-1}$. The inset shows the plot of $^{57}\text{Fe}-(T_1T)^{-1}$ against $^{75}\text{As}-(T_1T)^{-1}$ with the implicit parameter T ; $^{57}(T_1T)^{-1}/^{75}(T_1T)^{-1} \sim 0.68$.

A polycrystalline sample of ^{57}Fe -enriched $\text{Ba}_{0.6}\text{K}_{0.4}\text{Fe}_2\text{As}_2$ was synthesized by the high-pressure synthesis technique, as described elsewhere [22]. Powder X-ray diffraction measurements indicated that the $\text{Ba}_{0.6}\text{K}_{0.4}\text{Fe}_2\text{As}_2$ sample almost completely consisted of a single phase with the lattice parameters $a = 3.9142$ Å and $c = 13.305$ Å. The sample was moderately crushed into powder for the NMR measurements, which were easily performed under a strong magnetic field along the direction including the ab plane. The ^{57}Fe - and ^{75}As -NMR measurements were performed on a phase coherent pulsed NMR spectrometer at respective magnetic fields H of 11.966 and 5.12 T. T_1 was measured with a saturation recovery method.

Figure 1(a) shows the T dependence of the ^{57}Fe -NMR spectra at $H = 11.966$ T parallel to the ab plane. The Knight shift $^{57}K^{ab}$ stays almost constant above T_c , followed by a steep increase upon cooling below T_c , as shown in Fig. 1(b). The Knight shift comprises a spin component and an orbital component, denoted as K_s and K_{orb} , respectively. Note that $K_s = A_{hf}\chi_s(T)$ depends on T , but K_{orb} does not. Here, A_{hf} is the hyperfine coupling constant and $\chi_s(T)$ is the uniform spin susceptibility. Since $^{57}A_{hf}^{ab}$ is known to be negative due to the inner core-polarization effect, as in $\text{LaFeAsO}_{0.7}$ [23], the increase in $^{57}K^{ab}$ below T_c (see Fig. 1(b)) indicates the decrease in $\chi_s^{ab}(T)$, demonstrating the formation of a spin-singlet SC state, as in $\text{LaFeAsO}_{0.7}$. If we assume $^{57}K_{orb}^{ab} \sim 1.38$ % in this compound, $^{57}K_s^{ab}$ goes down to zero at $T = 0$, as displayed in Fig. 1(c).

$^{57}\text{Fe}/T_1$ was uniquely determined with a single component throughout the whole T range. A large enhancement of $^{57}\text{Fe}-(T_1T)^{-1}$ is observed on cooling down to T_c from the normal state, as also seen in the results for $^{75}\text{As}-(T_1T)^{-1}$ (Fig. 2). By contrast, note that $^{57}K_s^{ab}$, which is in proportion to $\chi_s(q=0, \omega=0)$, stays almost constant above T_c . In general, $(T_1T)^{-1}$ is expressed as

$$\frac{1}{T_1T} = \frac{\pi k_B \gamma_n^2}{(\gamma_e \hbar)^2} \sum_{\mathbf{q}} A_{hf}^2(\mathbf{q}) \frac{\chi''_{\perp}(\mathbf{q}, \omega_0)}{\omega_0},$$

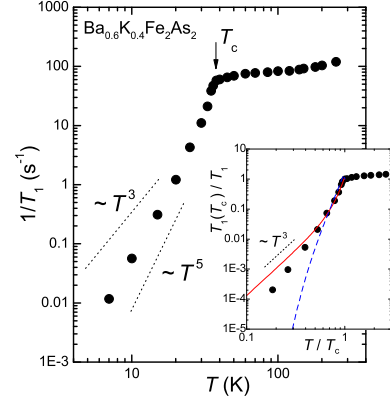


FIG. 3: (Color online) T dependence of $^{57}(1/T_1)$ for $\text{Ba}_{0.6}\text{K}_{0.4}\text{Fe}_2\text{As}_2$. The T dependence of $^{57}(1/T_1)$ exhibits a T^5 -like dependence well below T_c , which cannot be simulated with either a simple $d_{x^2-y^2}$ -wave model (solid curve) or an isotropic s -wave model with no coherence effect (dashed curve; see inset).

where $\chi''_{\perp}(\mathbf{q}, \omega_0)$ is the imaginary part of the dynamical susceptibility in a direction perpendicular to the applied magnetic field, ω_0 is the NMR frequency, and γ_n is the nuclear gyromagnetic ratio. The difference in T dependency between the Knight shift and $(T_1T)^{-1}$ points to the development of q -dependent spin fluctuations, except at $q = 0$, upon cooling. To unravel the characteristics of these spin fluctuations, compare the $(T_1T)^{-1}$ values at Fe and As sites; $^{57}\text{Fe}-(T_1T)^{-1}/^{75}\text{As}-(T_1T)^{-1} \sim 0.68$ and is almost constant in the range $T_c (= 38 \text{ K}) - 100 \text{ K}$, as shown in the inset of Fig. 2. If ferromagnetic spin fluctuations are predominant around $q = 0$, the ratio $^{57}(T_1T)^{-1}/^{75}(T_1T)^{-1} \simeq 0.038$ is estimated using $(^{57}A_{hf}/^{75}A_{hf})_{q=0}^2 \sim 1$. This value is about one order of magnitude smaller than the experimental value, indicating that ferromagnetic spin fluctuations are not developed. Furthermore, according to the argument in the literature [23], spin fluctuations around $\mathbf{Q} = (\pi, \pi)$ are not responsible for the large enhancement in $(T_1T)^{-1}$ values at both the Fe and As sites. Given these facts, it is likely that the enhancement is the results of the spin fluctuations with $\mathbf{Q} = (\pi, 0)$ and $(0, \pi)$ that would be expected from the interband nesting.

Here, we remark that on the basis of the fluctuation-exchange approximation (FLEX) on an effective five-band Hubbard model, the recent theoretical work [24] appears to explain qualitatively the evolution of magnetic characteristics from that in electron-doped systems to that in hole-doped systems: in electron-doped systems, $(T_1T)^{-1}$ and spin susceptibility decrease significantly upon cooling, producing a pseudogap behavior that originates from the band-structure effect, i.e., the existence of a high density of states just below the Fermi level. In hole-doped systems, $(T_1T)^{-1}$ is enhanced upon cooling due to the nesting across the disconnected FSs, but the Knight shift is not. In this model, it was

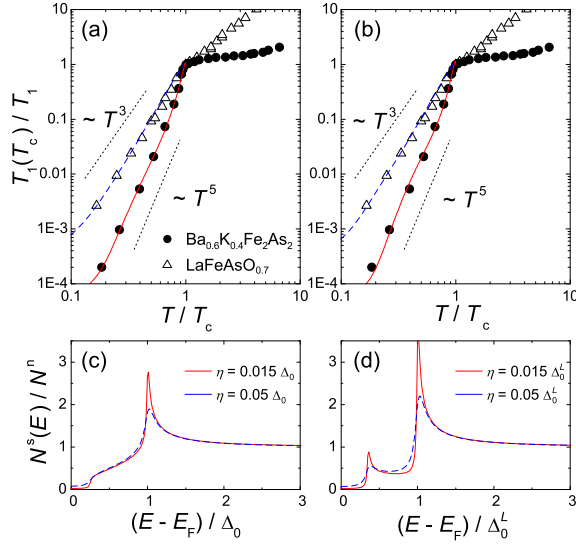


FIG. 4: (Color online) The simulations are based on (a) Model A and (b) Model B. The experimental ^{57}Fe - $1/T_1$ data for $\text{Ba}_{0.6}\text{K}_{0.4}\text{Fe}_2\text{As}_2$ and $\text{LaFeAsO}_{0.7}$ [23] are normalized by the value at T_c . Either model can qualitatively reproduce the experimental results, assuming reasonable fitting parameters (see Table I). The energy dependences of the density of states used in these simulations are based on (c) Model A and (d) Model B.

suggested that the dominant contribution to the pairing interaction for s^\pm -wave SC comes from an interplay between spin-dipole and spin-quadrupole and not from striped AFM spin fluctuations at $\mathbf{Q} = (\pi, 0)$ and $(0, \pi)$.

Next, we discuss the SC characteristics of $\text{Ba}_{0.6}\text{K}_{0.4}\text{Fe}_2\text{As}_2$ through the T dependence of ^{57}Fe - $1/T_1$, as shown in Fig. 3. In the SC state, ^{57}Fe - $1/T_1$ steeply decreases upon cooling, without a coherence peak just below T_c , pointing to the unconventional SC nature of this compound and electron-doped LaFeAsO systems [23]. On the other hand, ARPES revealed nearly isotropic and nodeless SC gaps with different values on three electron and hole FSs [10]. Motivated by these seemingly incompatible experimental results, an extended s^\pm -wave model with a sign reversal of the OP among the FSs has been proposed [11, 12, 13, 24]. Note that the T dependence of ^{57}Fe -($1/T_1$) below T_c cannot be simulated with either a simple $d_{x^2-y^2}$ -wave SC model ($\Delta(\phi) = \Delta_0 \cos 2\phi$ with $2\Delta_0/k_B T_c = 10$) or an isotropic s -wave model ($2\Delta_0/k_B T_c = 8$) with no coherence effect, as shown in the inset of Fig. 3. Therefore, we have applied a multiple SC gap model to interpret the T dependence of ^{57}Fe -($1/T_1$) below T_c .

First, we proceed with an analysis of $1/T_1$ by applying an anisotropic two-full-gap s^\pm -wave model in which one of the gaps is anisotropic and the other isotropic, denoted as Model A. This was proposed to explain the T^3 behavior of $1/T_1$ observed in $\text{LaFeAsO}_{0.6}$ on the basis of the effective five-band model [13]. For simplification, we assume that there are two FSs (FS1 and FS2) domi-

TABLE I: The sizes of the SC gaps, $N_{FS1}/(N_{FS1} + N_{FS2})$, and η/Δ_0 estimated by assuming Model A and Model B for $\text{Ba}_{0.6}\text{K}_{0.4}\text{Fe}_2\text{As}_2$ and $\text{LaFeAsO}_{0.7}$.

Model	Fitting parameters	$\text{Ba}_{0.6}\text{K}_{0.4}\text{Fe}_2\text{As}_2$ $T_c = 38$ K	$\text{LaFeAsO}_{0.7}$ $T_c^{H=0} = 28$ K
A	$2\Delta_0/k_B T_c$	9.2	4.6
	Δ_{\min}/Δ_0	0.25	0.25
	$N_{FS1}/(N_{FS1} + N_{FS2})$	0.4	0.4
	η/Δ_0	0.015	0.05
B	$2\Delta_0^L/k_B T_c$	9.4	4.4
	Δ_0^S/Δ_0^L	0.35	0.35
	$N_{FS1}/(N_{FS1} + N_{FS2})$	0.7	0.7
	η/Δ_0^L	0.015	0.05

nated by an isotropic full gap and an anisotropic full gap in the SC state, respectively, and neglect the coherence factor. These gap functions are given by $\Delta^{FS1} = \Delta_0$ and $\Delta^{FS2}(\phi) = (\Delta_0 + \Delta_{\min})/2 + (\Delta_0 - \Delta_{\min}) \cos 2\phi/2$. Here Δ_{\min} gives rise to an anisotropy in a full gap function, as described in Ref. [13]. According to Nagai et al., when we assume a fraction of the density of states (DOS) at FS1, $N_{FS1}/(N_{FS1} + N_{FS2}) = 0.4$, the experiment becomes consistent with a calculation using the parameters $\Delta_{\min} = 0.25 \Delta_0$, $2\Delta_0/k_B T_c = 9.2$, and the smearing factor $\eta = 0.015 \Delta_0$ for the DOS (to compensate for impurity scattering), as shown by solid line in Fig. 4(a). Here, N_{FS1} and N_{FS2} are the respective DOSs at FS1 and FS2. We state that this model reproduced the ^{57}Fe -($1/T_1$) result for $\text{LaFeAsO}_{0.7}$ using parameters $\Delta_{\min} = 0.25 \Delta_0$, $2\Delta_0/k_B T_c = 4.6$, and $\eta = 0.05 \Delta_0$, which is also shown by the dashed curve in Fig. 4(a). The $2\Delta_0/k_B T_c = 9.2$ in $\text{Ba}_{0.6}\text{K}_{0.4}\text{Fe}_2\text{As}_2$ is twice that in $\text{LaFeAsO}_{0.7}$ (4.6), which reveals that a strong-coupling SC state is realized in $\text{Ba}_{0.6}\text{K}_{0.4}\text{Fe}_2\text{As}_2$, thus increasing T_c . The fact that η in $\text{Ba}_{0.6}\text{K}_{0.4}\text{Fe}_2\text{As}_2$ is smaller than that in $\text{LaFeAsO}_{0.7}$ ($\eta^{\text{Ba122}}/\eta^{\text{La1111}} \simeq 0.3$) implies that the SC in $\text{Ba}_{0.6}\text{K}_{0.4}\text{Fe}_2\text{As}_2$ is more robust to impurity scattering because of the larger SC gap $2\Delta_0$. In Table I, we have summarized the experimentally obtained parameters for $\text{Ba}_{0.6}\text{K}_{0.4}\text{Fe}_2\text{As}_2$ and $\text{LaFeAsO}_{0.7}$. The important outcome is that the respective $1/T_1$ results for $\text{Ba}_{0.6}\text{K}_{0.4}\text{Fe}_2\text{As}_2$ and $\text{LaFeAsO}_{0.7}$, which seemingly follow a T^5 - and a T^3 -like behaviors below T_c , are consistently explained in terms of Model A only by changing the size of the SC gap $2\Delta_0$.

Next, since the ARPES experiment on $\text{Ba}_{0.6}\text{K}_{0.4}\text{Fe}_2\text{As}_2$ revealed that the anisotropy of the gap is small in every FS sheet [10], we tentatively apply an isotropic two-full-gap s^\pm -wave model in which both gaps are isotropic, denoted as Model B. Assuming that the large (Δ_0^L) and small (Δ_0^S) isotropic full gaps open on FS1 and FS2, respectively, a good fitting to the experiment is possible as shown by the solid line in Fig. 4(b) using parameters $2\Delta_0^L/k_B T_c = 9.4$, Δ_0^S/Δ_0^L

$= 0.35$, $N_{FS1}/(N_{FS1} + N_{FS2}) = 0.7$, and $\eta = 0.015$ Δ_0^L . However, the experiment does not replicate the slight step-wise behavior predicted by the calculation. Remarkably, the simulated result for the gap ratio $\Delta_0^S/\Delta_0^L = 0.35$ is comparable to the value estimated by ARPES (~ 0.44) [10]. As for $\text{LaFeAsO}_{0.7}$, we note that the $1/T_1$ data are also reproduced as shown by the dashed line in Fig. 4(b), using a smaller gap $2\Delta_0^L/k_B T_c = 4.4$ and a larger $\eta = 0.05$ Δ_0^L than those in $\text{Ba}_{0.6}\text{K}_{0.4}\text{Fe}_2\text{As}_2$. In this context, we cannot rule out at the present stage that Model B also explains both the experimental results in $\text{Ba}_{0.6}\text{K}_{0.4}\text{Fe}_2\text{As}_2$ and $\text{LaFeAsO}_{0.7}$. In order to shed light on the differences between the two models, the quasiparticle DOSs in the SC state are shown in Figs. 4(c) and 4(d), respectively. To identify the more appropriate model, further precise measurements are required on the hole-doped systems, involving systematic variation in the hole-doping level.

In conclusion, ^{57}Fe -NMR studies on the hole-doped $\text{Ba}_{0.6}\text{K}_{0.4}\text{Fe}_2\text{As}_2$ with $T_c = 38$ K have unraveled novel normal- and SC-state characteristics. Spin fluctuations with finite q -vectors develop upon cooling down to T_c ; they may originate from the nesting across the disconnected FSs with $\mathbf{Q} = (\pi, 0)$ and $(0, \pi)$. The ^{57}Fe -($1/T_1$) results have revealed that Model A is consistently applicable not only to hole-doped $\text{Ba}_{0.6}\text{K}_{0.4}\text{Fe}_2\text{As}_2$ with $T_c = 38$ K but also to electron-doped $\text{LaFeAsO}_{0.7}$ with $T_c = 24$ K. But Model B cannot be ruled out in understanding the present Fe-NMR results. In any case, the $2\Delta_0/k_B T_c$ value of $\text{Ba}_{0.6}\text{K}_{0.4}\text{Fe}_2\text{As}_2$ is almost twice that of $\text{LaFeAsO}_{0.7}$, which reveals that a strong coupling SC state is realized in $\text{Ba}_{0.6}\text{K}_{0.4}\text{Fe}_2\text{As}_2$. We suggest that the pairing mechanism of the unconventional SC with multiple fully gapped s^\pm -wave symmetry may be universal to the Fe-based superconductors.

This work was supported by a Grant-in-Aid for Specially Promoted Research (20001004) and partially supported by the Global COE Program (Core Research and Engineering of Advanced Materials-Interdisciplinary Education Center for Materials Science) from the Ministry of Education, Culture, Sports, Science and Technology (MEXT), Japan. M. Y. was supported by a Grant-in-Aid for Young Scientists (B) of MEXT (20740175).

[1] Y. Kamihara, T. Watanabe, M. Hirano, and H. Hosono, *J. Am. Chem. Soc.* **130**, 3296 (2008).
 [2] C. de la Cruz, Q. Huang, J. W. Lynn, J. Y. Li, W. Ratcliff II, J. L. Zarestky, H. A. Mook, G. F. Chen, J. L. Luo, N. L. Wang, and P. C. Dai, *Nature* **453**, 899 (2008).
 [3] D. J. Singh and M. H. Du, *Phys. Rev. Lett.* **100**, 237003 (2008).
 [4] Y. Nakai, K. Ishida, Y. Kamihara, M. Hirano, and H. Hosono, *J. Phys. Soc. Jpn.* **77**, (2008) 073701.
 [5] H.-J. Grafe, D. Paar, G. Lang, N. J. Curro, G. Behr,

J. Werner, J. Hamann-Borrero, C. Hess, N. Leps, R. Klingeler, and B. Büchner, *Phys. Rev. Lett.* **101**, 047003 (2008).
 [6] H. Mukuda, N. Terasaki, H. Kinouchi, M. Yashima, Y. Kitaoka, S. Suzuki, S. Miyasaka, S. Tajima, K. Miyazawa, P.M. Shirage, H. Kito, H. Eisaki, and A. Iyo, *J. Phys. Soc. Jpn.* **77**, 093704 (2008).
 [7] H. Luetkens, H.-H. Klauss, R. Khasanov, A. Amato, R. Klingeler, I. Hellmann, N. Leps, A. Kondrat, C. Hess, A. Kohler, G. Behr, J. Werner, and B. Büchner, *Phys. Rev. Lett.* **101**, 097009 (2008).
 [8] K. Hashimoto, T. Shibauchi, T. Kato, K. Ikada, R. Okazaki, H. Shishido, M. Ishikado, H. Kito, A. Iyo, H. Eisaki, S. Shamoto, and Y. Matsuda, *Phys. Rev. Lett.* **102**, 017002 (2009).
 [9] T. Kondo, A. F. Santander-Syro, O. Copie, Chang Liu, M. E. Tillman, E. D. Mun, J. Schmalian, S. L. Bud'ko, M. A. Tanatar, P. C. Canfield, and A. Kaminski, *Phys. Rev. Lett.* **101**, 147003 (2008).
 [10] H. Ding, P. Richard, K. Nakayama, K. Sugawara, T. Arakane, Y. Sekiba, A. Takayama, S. Souma, T. Sato, T. Takahashi, Z. Wang, X. Dai, Z. Fang, G. F. Chen, J. L. Luo, and N. L. Wang, *Europhys. Lett.* **83**, 47001 (2008).
 [11] I.I. Mazin, D. J. Singh, M. D. Johannes, and M. H. Du, *Phys. Rev. Lett.* **101**, 057003 (2008).
 [12] K. Kuroki, S. Onari, R. Arita, H. Usui, Y. Tanaka, H. Kontani, and H. Aoki, *Phys. Rev. Lett.* **101**, 087004 (2008).
 [13] Y. Nagai, N. Hayashi, N. Nakai, H. Nakamura, M. Okumura, and M. Machida, *New J. Phys.* **10**, 103026 (2008).
 [14] M. Rotter, M. Tegel, and D. Johrendt, *Phys. Rev. Lett.* **101**, 107006 (2008).
 [15] M. Rotter, M. Tegel, D. Johrendt, I. Schellenberg, W. Hermes, and R. Pöttgen, *Phys. Rev. B* **78**, 020503(R) (2008).
 [16] Q. Huang, Y. Qiu, W. Bao, M. A. Green, J. W. Lynn, Y. C. Gasparovic, T. Wu, G. Wu, and X. H. Chen, *Phys. Rev. Lett.* **101**, 257003 (2008).
 [17] H. Fukazawa, T. Yamazaki, K. Kondo, Y. Kohori, N. Takeshita, P. M. Shirage, K. Kihou, K. Miyazawa, H. Kito, H. Eisaki, and A. Iyo, *J. Phys. Soc. Jpn.* **78** 033704 (2009).
 [18] H. Mukuda, N. Terasaki, M. Yashima, H. Nishimura, Y. Kitaoka, and A. Iyo: *Physica C Special Edition on Superconducting Pnictides*, in press.
 [19] K. Terashima, Y. Sekiba, J. H. Bowen, K. Nakayama, T. Kawahara, T. Sato, P. Richard, Y.-M. Xu, L. J. Li, G. H. Cao, Z.-A. Xu, H. Ding, and T. Takahashi, arXiv:0812.3704v1.
 [20] S. Kawasaki, K. Shimada, G. F. Chen, J. L. Luo, N. L. Wang, and Guo-qing Zheng, *Phys. Rev. B*, **78** 220506(R) (2008).
 [21] K. Matano, G.L. Sun, D.L. Sun, C.T. Lin, and G.-q. Zheng, arXiv:0903.5098v1.
 [22] P. M. Shirage, et al. arXiv:0903.3515.
 [23] N. Terasaki, H. Mukuda, M. Yashima, Y. Kitaoka, K. Miyazawa, P.M. Shirage, H. Kito, H. Eisaki, and A. Iyo, *J. Phys. Soc. Jpn.* **78** 013701 (2009).
 [24] H. Ikeda, *J. Phys. Soc. Jpn.* **77**, 123707 (2008).
 [25] F. Ning, K. Ahilan, T. Imai, A. S. Sefat, R. Jin, M. A. McGuire, B. C. Sales, and D. Mandrus: *J. Phys. Soc. Jpn.* **78** (2009) 013711.